

**A bovine antibody possessing an ultralong complementarity-determining region
CDRH3 targets a highly conserved epitope in *sarbecovirus* spike proteins**

Matthew J. Burke, James N.F. Scott, Thomas C. Minshull, Zeqian Gao, Iain Manfield, Sinisa Savic, Peter G. Stockley, Antonio N. Calabrese and Joan Boyes

Figure S1. Estimation of scFv library diversity.

Figure S2. Lentivirus transduction of scFv library.

Figure S3. Isolation of an ultralong scFv that binds to the wildtype SARS-CoV-2 Spike and receptor binding domain.

Figure S4. Purified B9-scFv binds to SARS-CoV-2 Spike expressed on the surface of 293T cells.

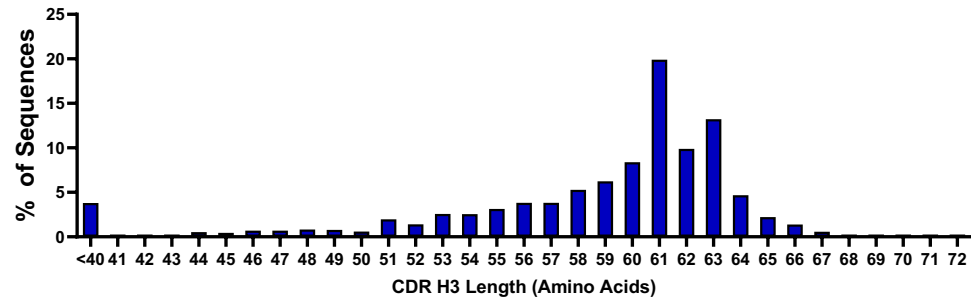
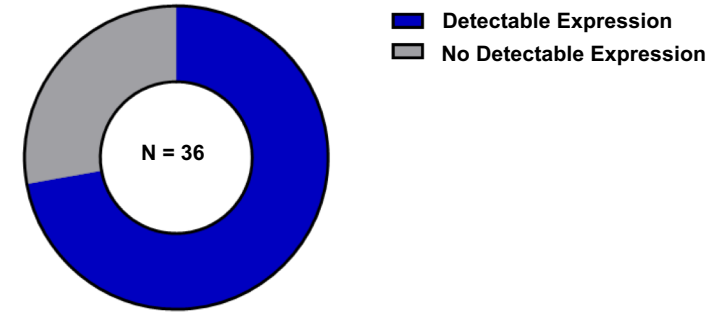
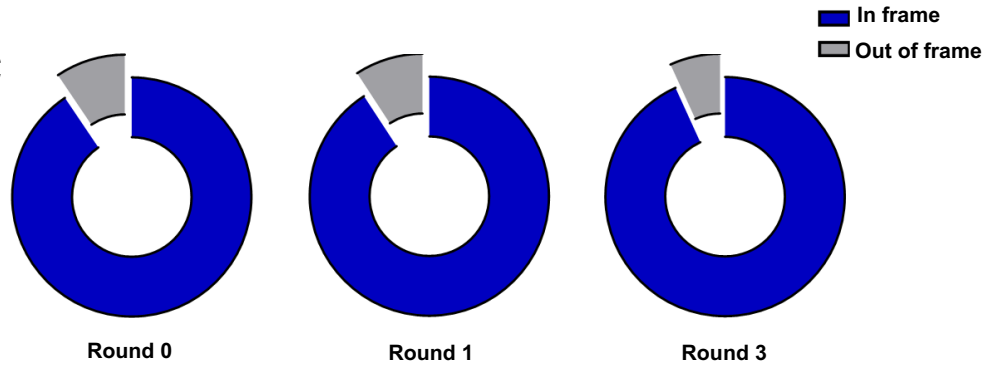
Figure S5. Hydrogen-deuterium exchange experiments for epitope localisation.

Figure S6. Localising the epitope of B9-scFv to a cryptic site by hydrogen-deuterium exchange and site-directed mutagenesis.

Figure S7. Mutagenesis of the B9 knob domain.

Table S1: Nucleotide sequences in the expression cassette.

Table S2: HDX Data Summary Table.

A**B****C**

	Round 0	Round 2	Round 3
Unique	3168	379	250
Non-unique	N/A	260	102

Estimated Library Size	
Round 2	Round 3
4617	7764

Figure S1. Estimation of scFv library diversity. *A*, Histogram showing the proportion of heavy chain amino acid sequences with CDRH3 between 40 and 72 amino acids. Heavy chain amino acid sequences were determined from the amplicon sequencing of the Round 0 plasmid scFv library. *B*, Random pBovShow-scFv clones were ($n = 36$) transfected into 293Ts and tested for cell-surface expression. The positive fraction is indicated in blue. *C*, Clonotypes were assembled from amplicon sequencing of the scFv plasmid library at three different time points during the Spike-binding enrichment (Round 0, Round 2 and Round 3). The resultant clonotype assemblies were used to assess the fraction of productive and non-productive heavy chain sequences.

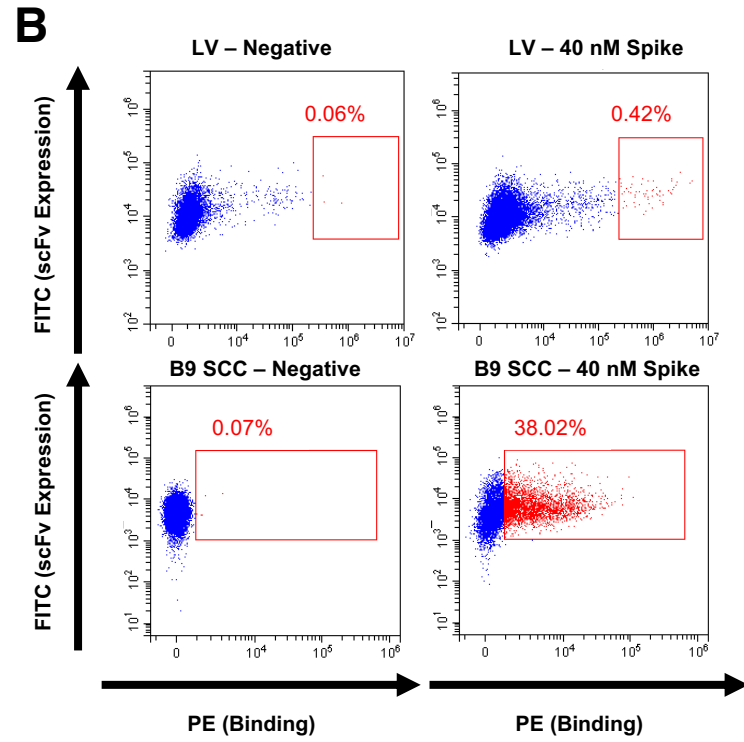
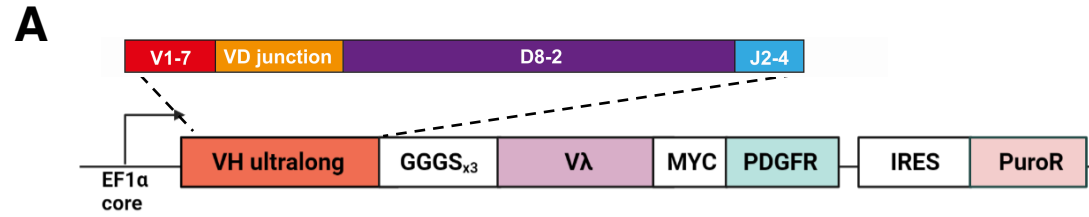


Fig. S2

Figure S2. Lentivirus transduction of scFv library. *A*, Cartoon showing the cloning of the enriched ultralong V_H library into the lentivirus vector used to generate stable cell lines. *B*, Upper: FACS plots showing stable polyclonal 293T cells transduced with enriched lentivirus scFv library incubated without (left) and with (right) 40 nM Spike. Lower: Single cell clone (SCC) B9-scFv incubated without (left) and with (right) 40 nM Spike. The red boxes show cells that express scFvs that bind Spike.

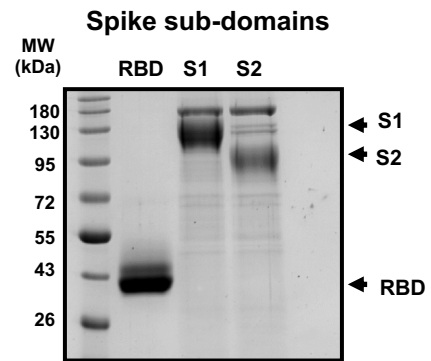
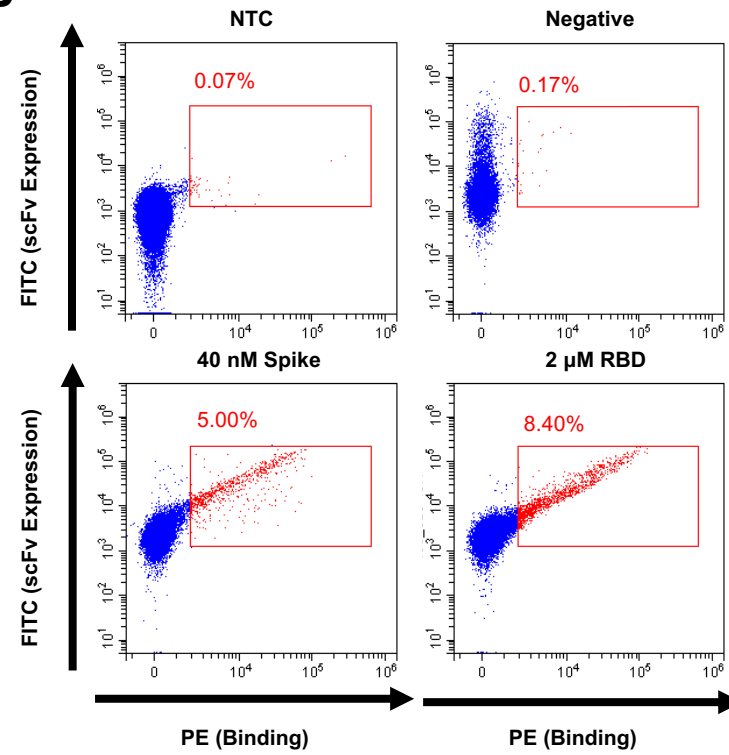
A**B**

Figure S3. Isolation of an ultralong scFv that binds to the wildtype SARS-CoV-2 Spike and receptor binding domain. *A*, SDS-PAGE of purified SARS-CoV-2 Spike sub-domains. *B*, FACS plots showing, Upper: non-transfected 293T cells (left) and 293T cells transfected with B9-scFv (right). Lower: 293T cells transfected with B9-scFv and incubated with 40 nM Spike (left) or 2 μ M RBD (right).

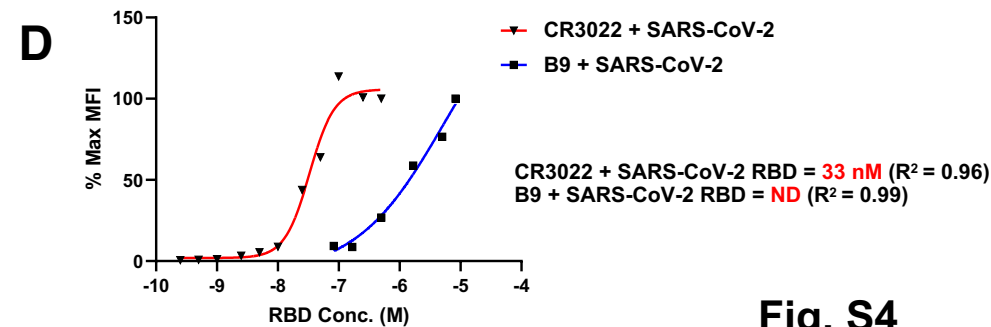
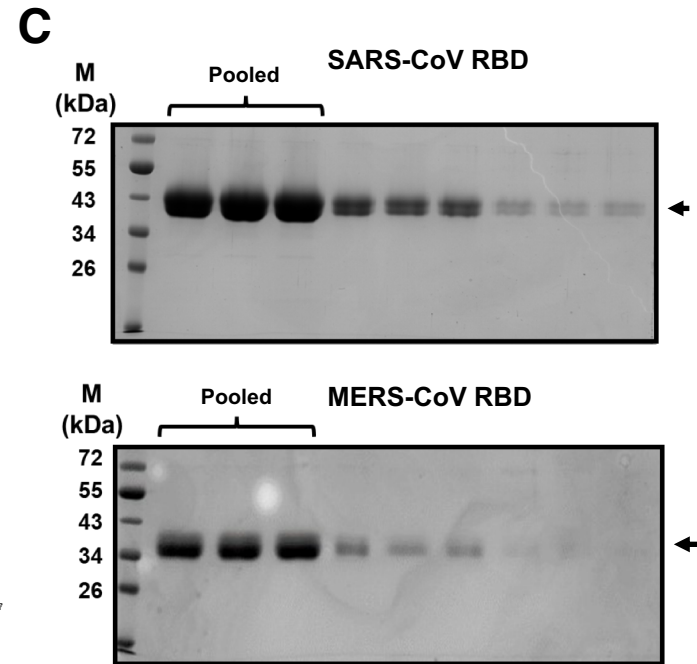
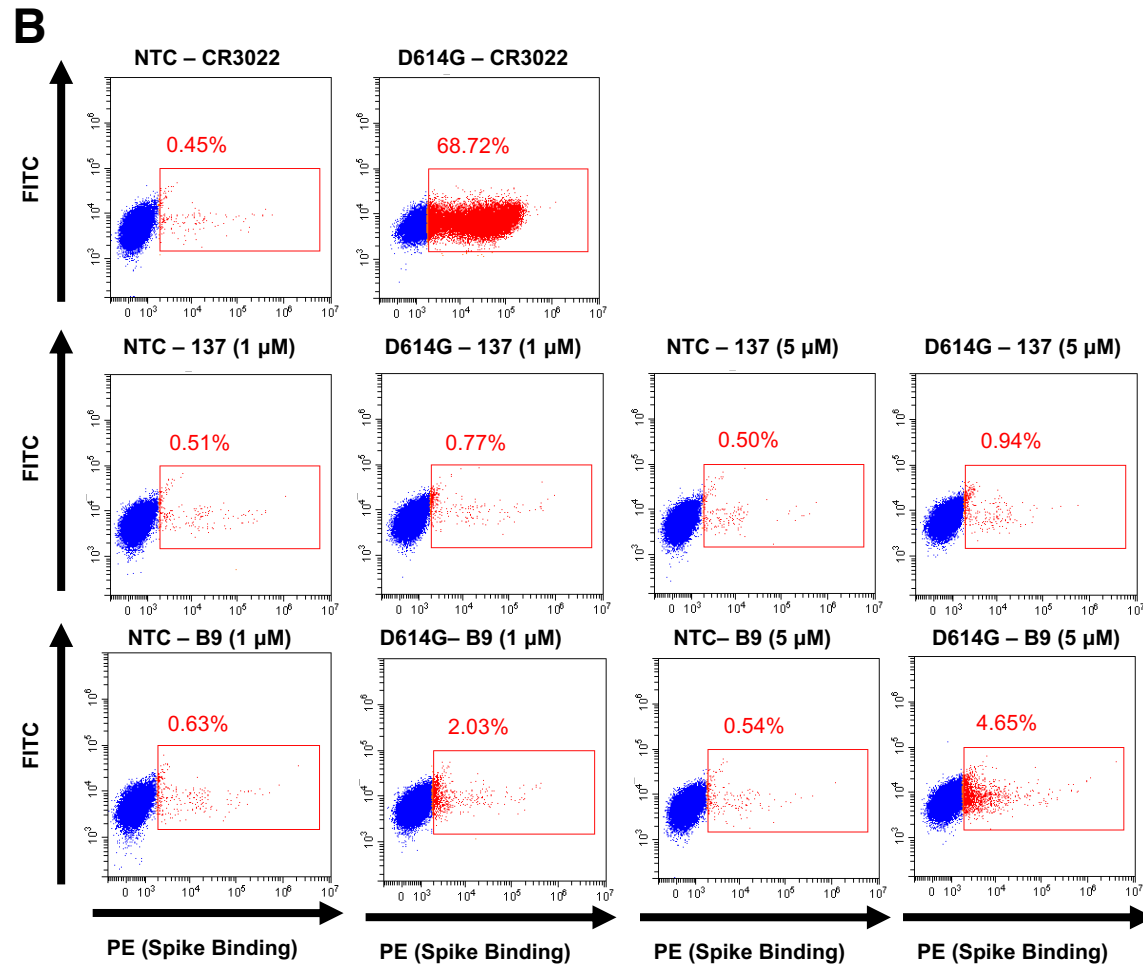
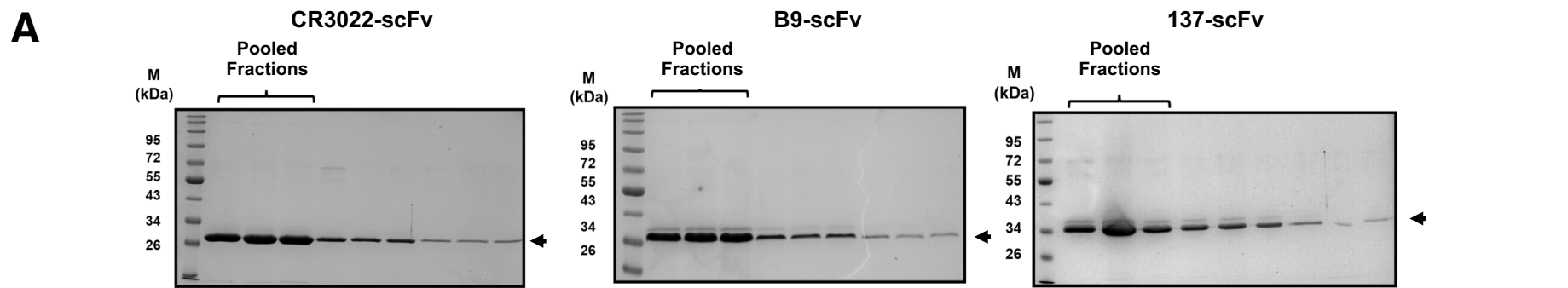


Fig. S4

Figure S4. Purified B9-scFv binds to SARS-CoV-2 Spike expressed on the surface of 293T cells. *A*, SDS-PAGE gels of purified CR3022-, 137- and B9-scFvs. *B*, Upper: FACS plots showing non-transfected (NTC) and 293T cells expressing SARS-CoV-2 Spike (Wu-Hu-1+D614G) incubated with 200 nM CR3022-scFv to confirm cell surface Spike localization. Middle & lower: FACS plots showing non-transfected (NTC) and 293T cells expressing SARS-CoV-2 Spike protein (Wu-Hu-1+D614G) incubated with 1 and 5 μ M 137-scFv (middle; negative control) or 1 and 5 μ M B9-scFv (lower). Red box indicates scFv binding to 293T cells. *C*, SDS-PAGE of purified SARS-CoV (upper) and MERS-CoV (lower) RBD. *D*, 293T cells were transfected with B9-scFv or CR3022-scFv and incubated with increasing amounts of purified SARS-CoV-2 RBD. Estimated K_D and R^2 values are indicated.

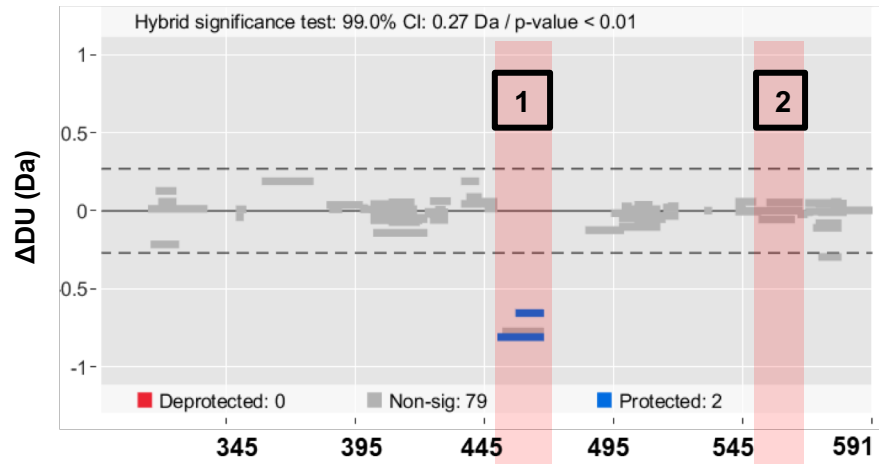
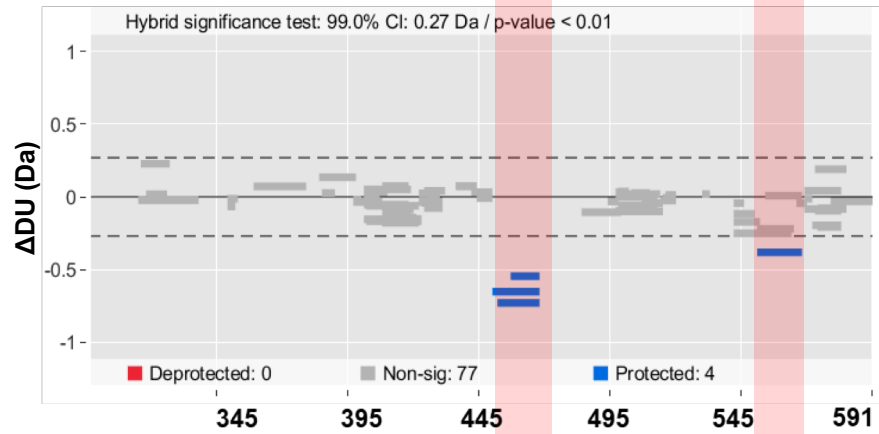
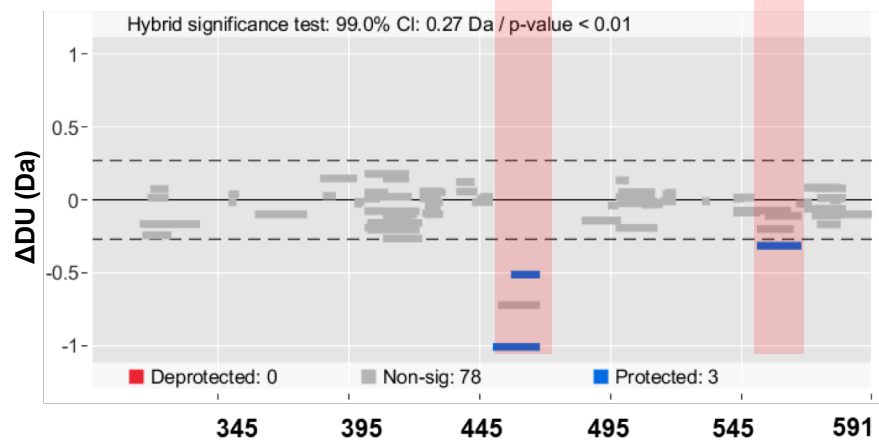
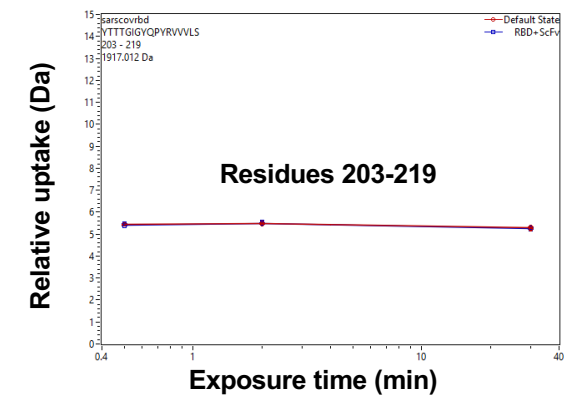
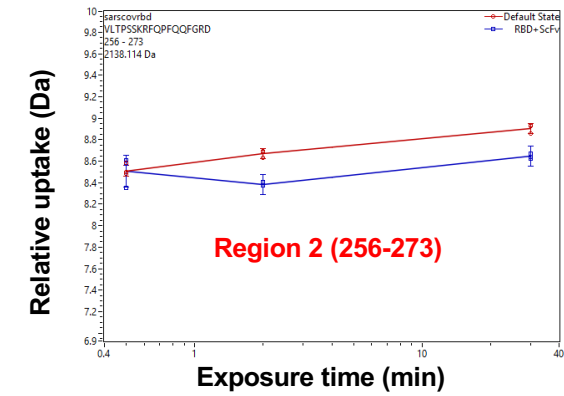
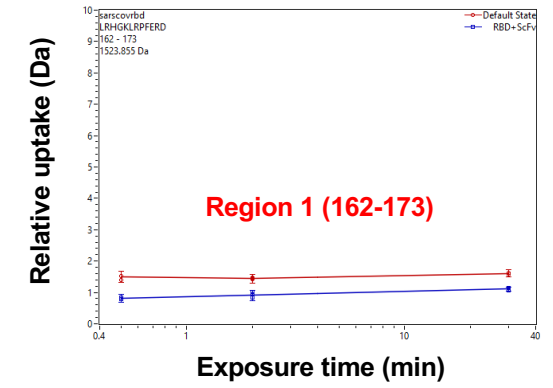
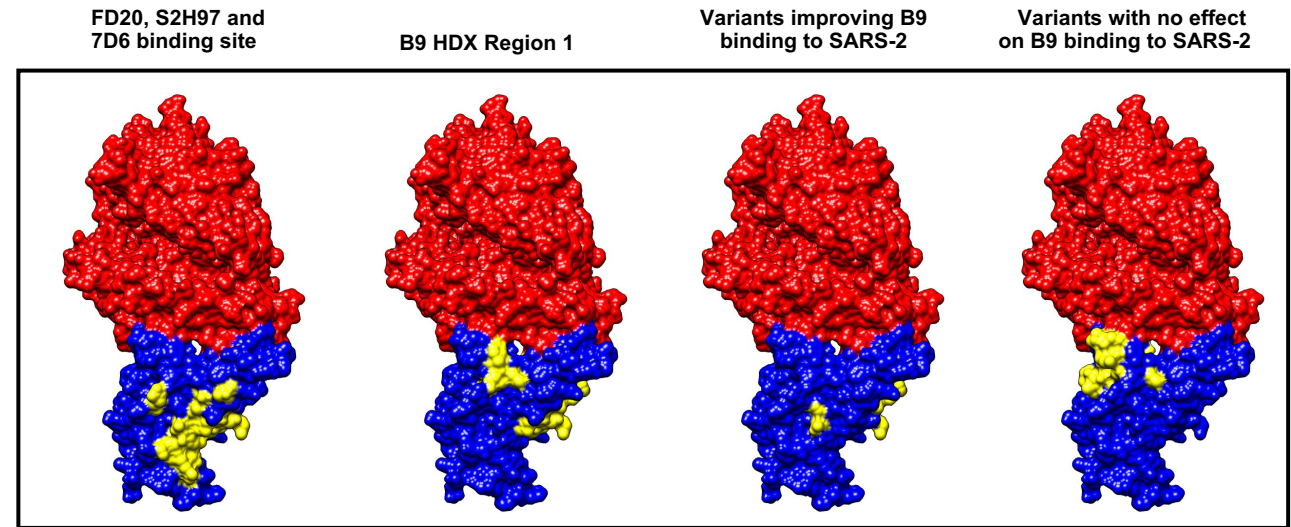
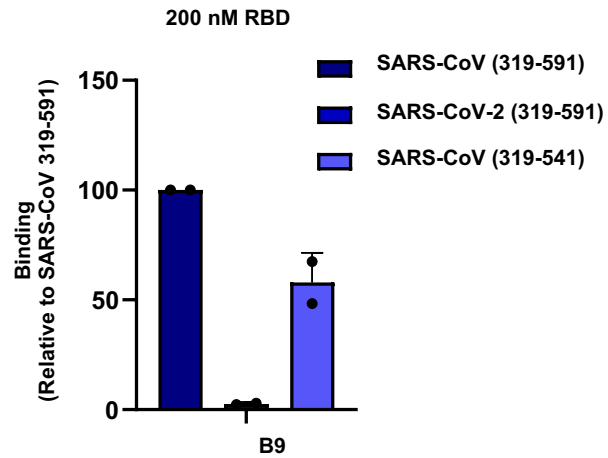
A**0.5 minute exposure****2-minute exposure****30-minute exposure****B****Fig. S5**

Figure S5. Hydrogen-deuterium exchange experiments for epitope localisation. *A*, Wood's plots showing the differences in deuterium uptake in SARS-CoV RBD at 0.5, 2 and 30 minutes of exposure to deuterium, comparing RBD alone to RBD in the presence of B9-scFv. Wood's plots were generated using Deuterios. Peptides coloured in blue are protected from exchange in the presence of B9-scFv and cluster to two regions (labelled 1 and 2 and highlighted in red). Peptides with no significant difference between conditions, determined using a 99% confidence interval (dotted line), are shown in grey. For each time point and condition, three replicate measurements were performed. *B*, Representative deuterium uptake plots of peptides derived from the RBD in region 1 (top), region 2 (middle) and a region where no protection from exchange was observed (bottom). Data are shown as mean \pm standard deviation ($n = 3$).

A

Protein	Start	End	Peptide	State	Average uptake difference	Standard Deviation
SARS-CoV-RBD	449	467	YNYKYRYLRHGKLRPFERD	RBD + B9-scFv	-0.6526	0.0411
SARS-CoV-RBD	452	467	YKYRYLRHGKLRPFERD	RBD + B9-scFv	-0.7301	0.1911
SARS-CoV-RBD	456	467	LRHGKLRPFERD	RBD + B9-scFv	-0.5460	0.0810
SARS-CoV-RBD	551	565	VLTPSSKRFQPFQQFGRD	RBD + B9-scFv	-0.3821	0.0924

B**C****D**

Mutations
A348P
N354E
P384A
Mut402-406 (I402V, R403K, E406D)
I434L
Mut438-447 (S438T, N439R, L441I, S443A, K444T, V445S, G446T)
L452K
Mut455-462 (L455Y, F456L, K458H, S459G, N460K, K462R)

Figure S6. Localising the epitope of B9-scFv to a cryptic site by hydrogen-deuterium exchange and site-directed mutagenesis. *A*, Peptides of SARS-CoV RBD protected from deuterium uptake in the presence of B9-scFv following a 2-minute exposure to deuterated buffer. *B*, Surface maps of monomeric SARS-CoV-2 RBD (Blue) bound to hACE2 (red) generated using UCSF Chimera (PDB: 6M0J). Regions of interest are highlighted in yellow. There is significant overlap between the footprints of FD20, S2H97 and 7D6 with the proposed epitope of B9. *C*, 293T cells expressing B9-scFv on the cell surface were incubated with 200 nM of the recombinant RBD proteins shown. Binding was measured as the mean fluorescence intensity (MFI) and is presented relative to SARS-CoV (319-591). Data presented are mean \pm SEM ($n = 3$). *D*, SARS-CoV-2 to SARS-CoV mutations tested in Fig. 5C and *D*.

A

B9-WT CTTVHQ**RD**SCPYDSSHSQY**C**SYGW**SC**GVY**NC**RPVAVWYRYG**SC**GT**C**DNLF**S**YVDAW
 B9-Mut1 CTTVHQ**RD**SC**PETYYG**S**GL**C**S**YGW**SC**GVY**NC**RPVAVWYRYG**SC**GT**C**DNLF**S**YVDAW
 B9-Mut2 CTTVHQ**RD**SCPYDSSHSQY**C****ETYYG**C**SGL**NC**R**PAVWYRYG**SC**GT**C**DNLF**S**YVDAW
 B9-Mut3 CTTVHQ**RD**SCPYDSSHSQY**C**SYGW**SC**GV**ETC****YYG**S**GL**RYG**SC**GT**C**DNLF**S**YVDAW
 B9-Mut4 CTTVHQ**RD**SCPYDSSHSQY**C**SYGW**SC**GVY**NC**RPVAV**AAAAG**SCGT**C**DNLF**S**YVDAW

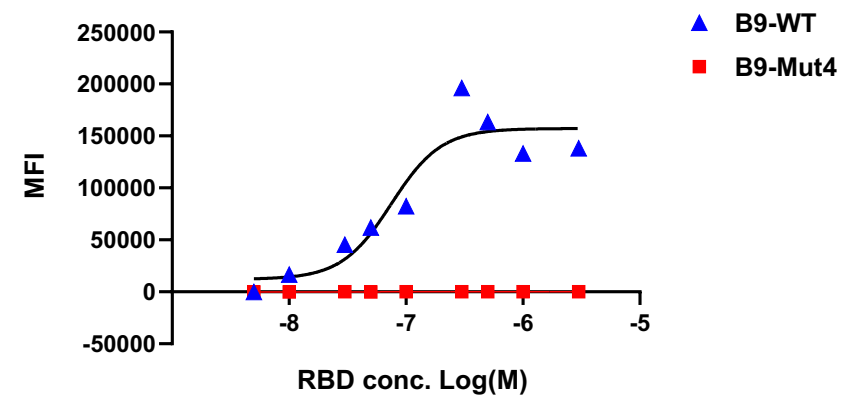
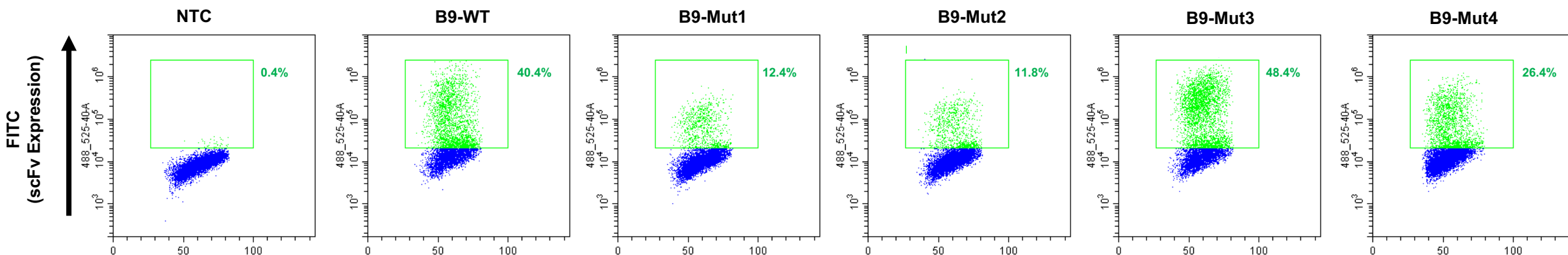
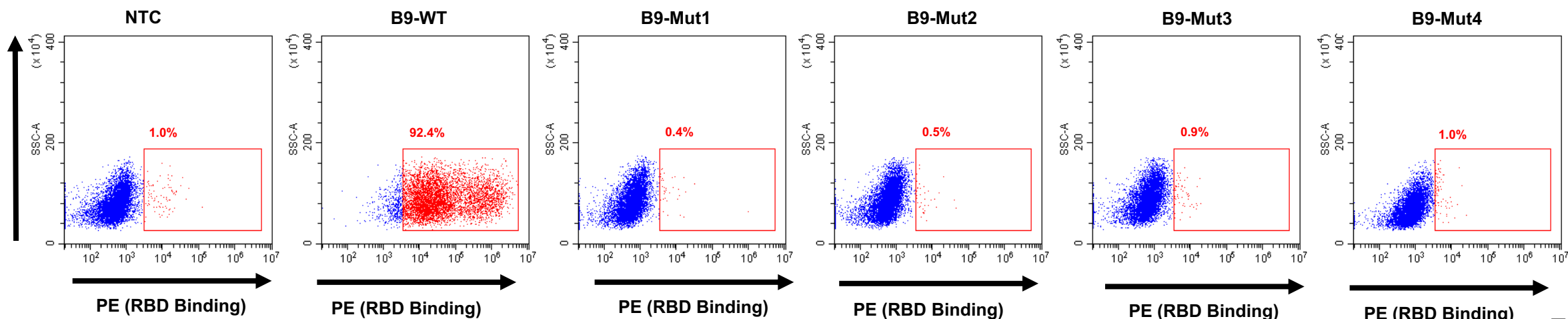
D**B****C**

Figure S7. Mutagenesis of the B9 knob domain. *A*, B9 knob domain mutations tested for expression and RBD binding in (*B*). VH1-7, blue; VD junction, orange; DH8-2, black; JH2-4, green. Cysteines are highlighted in yellow, while amino acids mutated in B9-Mut1-4 are in red. *B,C* FACS plots showing the expression of B9-WT and B9-Mut1-4 scFvs (*B*) and their binding to 200 nM SARS-CoV RBD (*C*) as measured by FACS. SSC refers to side scatter. *D*, Binding of B9-WT and B9-Mut4 to a titration of SARS-CoV RBD (5 – 3000 nM). Binding is presented as mean fluorescence intensity (MFI). All samples were stained with α -Myc-FITC and α -His-PE (1:100) prior to analysis by flow cytometry. Expression (FITC) and binding (PE) are shown separately to improve clarity.

Table S1: Nucleotide sequences in the expression cassette.

Name	Sequence
pBovshow cassette	ATGGAGACAGACACACTCCTGCTATGGGTA CTGCTGCTCTGGGTTCCAGGTTCCACTGGT GACGCTGCTAGA- HeavyChain - GGGATCTGGGGTGGTGGTTCTGGTGGTGG TGGTTCTGGTGGTGGTGGTTCTTCGCGAGC C-LightChain - GAGGTCGACGAACAAAACTCATCTCAGAA GAGGATCTGAATGCTGTGGGCCAGGACAC GCAGGAGGTCATCGTGGTGCCACACTCCTT GCCCTTTAAGGTGGTGGTGGTGGTGGTGGT CCTGGCCCTGGTGGTGGTGGTGGTGGTGGT CCTTATCATCCTCATCATGCTTTGGCAGAAG AAGCCACGTTAG
B9 Heavy chain variable domain	CAGGTGCAGCTGCGGGAGTCGGGCCCCAG CCTGGTGAAGCCCTCACAGACCCTCTCGCT CACCTGCACGGCCTCTGGATTCTCATTGAG CGACAAGGCTGTAGGCTGGGTCCGCCAGG CTCCAGGGAAGGCGCTGGAGTGGCTCGGT GGTATAGACACTGGTGGGAAGCACAGGCTAT AACCCAGGCCTGAAATCCCGGCTCAGCATC ACCAAGGACAACCTCCAAGAGCCAAATCTCT CTGTCAGTGAGCAGCGTGACAACCTGAGGA CTCGGCCACGTACTIONACTGTACTIONACTG CCAACGAGATAGTTGTCCTTATGATAGTAG CCATTCTCAGTACTGTTCTTACGGTTGGAGT TGTGGTGTAACTGTCGGCCTGCTGTTT GGTATCGTTATGGTTCTTGTGGTACTTGTGA TAATTTGTTCTCGTACGTCGATGCCTGGGG CCAAGGACTCCTGGTCACCGTCTCCTCAGG G
Vλ Light chain variable domain	CAGGCTGTGCTGAATCAGCCATCATCCGTG TCCGGGTCCCTGGGCCAGAGGGTCTCCAT CACCTGCTCTGGAAGCAGCAGCAATGTTGG AAATGGATATGTGAGCTGGTACCAACTGAT CCCAGGATCGGCCCCAGAACCTCATCTA TGGTGACACCAGTCGAGCCTCGGGGGTCC CCGACCGATTCTCCGGCTCCAGGTCTGGG AACACAGCCACCCTGACCATCAGCTCGCTC CAGGCTGAGGACGAGGCAGATTATTTCTGT GCATCTGCTGAGGATAGTAGCAGTAATGCT GTTTTCGGCAGCAGGACCACACTGACCGTC CTGCTC

Table S2: HDX Data Summary Table. SD = standard deviation, CI = confidence interval.

Data Set	SARS-CoV RBD	SARS-CoV RBD + B9-scFv
HDX reaction details	50 mM potassium phosphate, pD 8, 0.3 M NaCl, 4 °C	50 mM potassium phosphate, pD 8, 0.3 M NaCl, 4 °C
HDX time course (min)	0.5, 2, 30 min	
HDX control samples	Maximally labeled controls were not performed.	
Back-exchange	~ 30 %	
# of Peptides	81	81
Sequence coverage	75.67%	75.67%
Average peptide length / Redundancy	11.04 / 3.94	11.04 / 3.94
Replicates (biological or technical)	3 (technical)	3 (technical)
Repeatability	0.0476 (average SD)	0.0465 (average SD)
Significant differences in HDX (delta HDX > X D)	Reference	Hybrid Significance test: 99% CI: 0.27Da/ p-value <-0.01